JI EUN LEE[1], SOO BIN BAE[1], NAM CHOON CHO[1], HYUNG IK LEE[1*],
ZICHENG MENG[2], KEE SUNG LEE[2*]

EVALUATING THE DURABILITY OF SiC-COATED CARBON COMPOSITES UNDER THERMAL SHOCK CONDITIONS

Oxidation and indentation properties of silicon carbide-coated carbon composites were investigated to analyze its durability under atmospheric thermal shock conditions. The silicon carbide-coated samples were prepared either with chemical vapor deposition or chemical vapor reaction/chemical vapor deposition hybrid coating. The remnant weight of uncoated and coated samples was investigated after each thermal shock cycle. The surface and cross-section of coated samples were then analyzed to confirm morphological changes of the coating layers. The spherical indentation test for uncoated and coated samples were also performed. As a result, silicon carbide coating improved the oxidation resistance, elastic modulus, and hardness of carbon composites. Hybrid coating drastically enhanced the durability of samples at high temperature in atmospheric conditions.

Keywords: durability, carbon composites, silicon carbide coating, chemical vapor deposition, chemical vapor reaction

1. Introduction

Carbon composites have excellent thermal shock resistance and good mechanical properties at elevated temperatures and non-oxidizing environments. However, carbon composites rapidly oxidize above 500°C in atmospheric conditions, which restricts their application in civil and military fields [1,2]. Therefore, methods such as ceramic coating were studied to improve the oxidation resistance of carbon composites at high temperatures. Silicon carbide (SiC) is a potential material for ceramic coating owing to its good thermal stability and compatibility with carbon composites [3]. SiC-coated composites have high hardness and chemical stability, which are directly related to erosion resistance properties [4].

In our previous report, we suggested an effective coating method via a combination of chemical vapor reaction (CVR) and chemical vapor deposition (CVD) processes to protect carbon composites against high-temperature oxidative torch flame [5]. However, to estimate service life and wear resistance at certain temperatures, it is necessary to perform the thermal shock test with microstructural and mechanical analysis [6].

In this study, SiC-based deposition of dense and high-quality coating on carbon composites via CVD or CVR/CVD processes was conducted. The thermal shock tests were per-formed to evaluate the durability of composites in high oxidative surroundings. The measured weight change was compared with that of original carbon composites after each cycle. The mechanism of crack-formation and delamination of the coating layer was investigated to evaluate thermal durability of the samples. In addition, investigating mechanical properties such as relative elastic modulus and hardness provided an estimate for the wear resistance of composites.

2. Experimental

2.1. Preparation of samples

Carbon composites with 1.6 g/cm^3 density were manufactured by the needle punch process and densification process with impregnation and carbonization conducted at atmospheric pressure using a coal tar pitch. The carbon composites were shaped to a size of Ø30×5 mm to characterize the durability of the coating.

The SiC coating process was performed on both sides of composites through the CVR and CVD processes. The coating conditions were presented in our previous article [5]. Two kinds of coating samples were prepared and designated as D and RD.

1   AGENCY FOR DEFENSE DEVELOPMENT, YUSEONG P.O. BOX 35, DAEJEON, 34186, KOREA
2   KOOKMIN UNIVERSITY, SCHOOL OF MECHANICAL ENGINEERING, JEONGNEUNG-RO 77, SEONGBUK-GU, SEOUL, 02707, KOREA

*   Corresponding authors: hyungic7575@gmail.com; keeslee@kookmin.ac.kr

Sample D and RD indicate the 2 cycles of the CVD and 1 cycle of the CVR processes performed on the composites, respectively. For sample RD, 2 cycles of the CVD process were applied after CVR. The sample names according to coating methods are summarized in Table 1.

TABLE 1

Name of samples

Sample name	Coating method
C/C	uncoated
D	CVD (2 cycles)
RD	CVR (1 cycle) + CVD (2 cycles)

2.2. Experiment and characterization

The thermal shock test was performed using a heating furnace (Ajeon Industry, Korea) in atmospheric conditions to evaluate the durability of coating layers. The test was performed in triplicate for each sample type. Samples were embedded in the Al_2O_3 crucible, packed with Al_2O_3 powder, and loaded in the heating furnace. The furnace temperature was increased to 1500°C at a heating rate of 5°C/min, then maintained for 1 h and cooled to room temperature. This cycle was repeated 5 times, and the weight remnant ratio of samples was calculated for each cycle [7]. The morphologies of SiC coated samples before and after the thermal shock test were analyzed using scanning electron microscopy (SEM) (Quanta FEG 650). Energy-dispersive X-ray spectroscopy (EDS) analysis was also performed.

To evaluate the mechanical properties, the spherical indentation test was performed on the surface of uncoated carbon composites and the SiC-coated composites before and after the thermal shock cycles. During the spherical indentation test, a constant indentation load (P, 500 N) was applied on each sample using a tungsten carbide (WC) ball with a radius (r) of 3.18 mm to obtain an indentation load-displacement (h) curve. The crosshead speed was 0.2 mm/min during loading and unloading, and the test was performed in atmospheric conditions [7,8]. The elastic modulus is determined by drawing a tangent slope (dP/dh) at 80 % of the maximum load in the unloading curve. The hardness is determined by the residual displacement (h_p) (Fig. 4). The relative elastic modulus and the relative hardness was obtained by dividing values of D and RD with the original value of C/C, before and after the test, respectively.

3. Results and discussion

Fig. 1 shows the changes in the weight remnant ratio during the thermal shock test through images of coated composites after 5 cycles of testing. As the tests were performed, the weight remnant ratio of samples decreased with each cycle. The crack was more clearly visible on the surface of D than on RD. Uncoated carbon composites samples nearly disappeared after the test; two samples were completely oxidized and only 0.01 wt.% of the other sample remained. The weight remnant ratio of coated samples, D and RD, was 77.91% and 97.08%, respectively. Hence, the SiC coating layer effectively prevented the oxidation of carbon composites. Furthermore, using CVR to apply the interlayer of SiC coating could enhance the thermal protection properties of samples in oxidative surroundings.
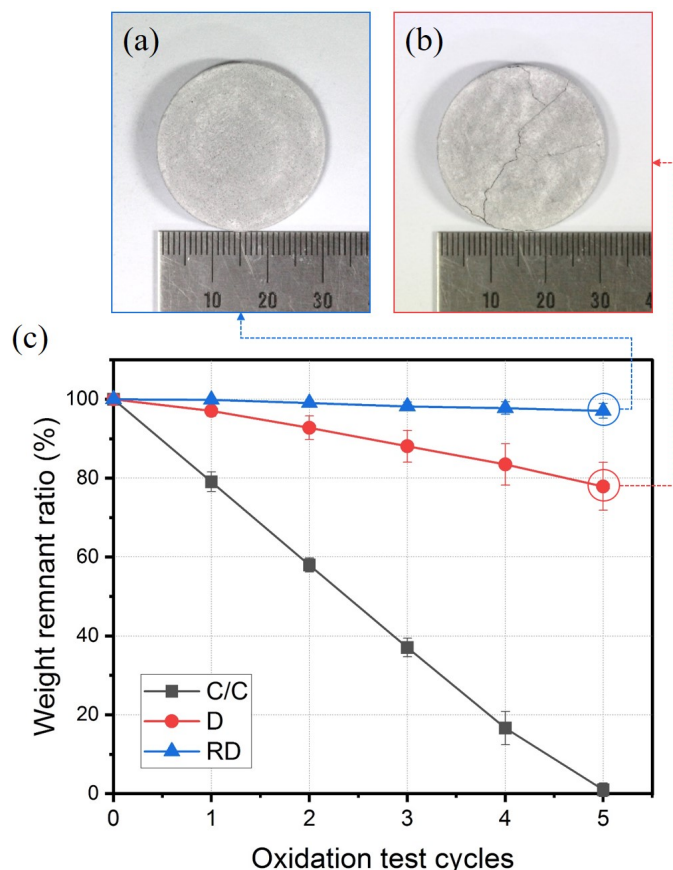

Fig. 1. Photo images after 5 cycles of the thermal shock test: (a) RD, (b) D, and (c) curves of weight remnant ratio as a function of oxidation test cycles

To analyze the prevention of oxidation, surface and cross-sectional micro-scale SEM images were obtained before and after the thermal shock test. Fig. 2 shows the surface morphologies of SiC-coated samples before and after the test. Before the thermal shock test, the crack width of D and RD was 1-5 and 1-3 μm, respectively. The variation in crack width was due to a mismatch in the thermal expansion coefficients of carbon and SiC [9]. After the thermal shock test, the crack width of D was 60-80 μm, as seen from Fig. 2(c). However, in Fig. 2(d), the crack width of RD was 4-7 μm, showing little change in crack width than that of the original RD. The coating layer of RD preserved the shape of composites during the thermal shock test.

Fig. 3 shows the cross-sectional SEM/EDS images of coated samples before and after the thermal shock test. SEM analysis was performed in the backscattered electrons mode to discern coating layer/substrate interface. In Fig. 3(a) and Fig. 3(b),
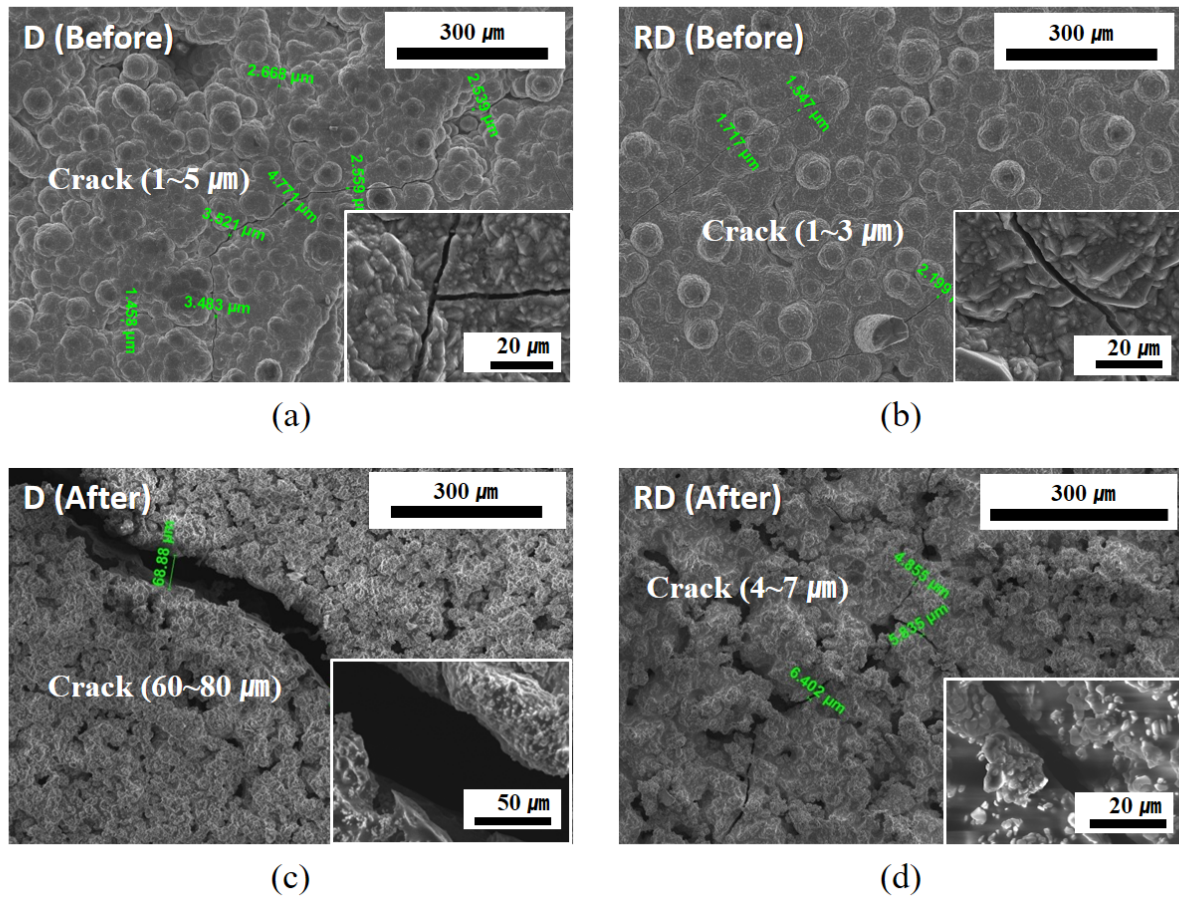
Fig. 2. Surface SEM images of coated samples before/after the thermal shock test: (a) D and (b) RD before the test, and (c) D and (d) RD after the test

SiC phases were formed by CVR and CVD processes and the lengths of SiC coating layer of D and RD were 80-110 μm and 100-140 μm, respectively. After thermal shock test, SiC phases transformed to SiO_2 layer due to thermal oxidization [10]. The formation of SiO_2 was confirmed by EDS analysis as shown in Fig. 3(c) and Fig. 3(d). In those Figures, Aluminum phases were detected due to the test environment, and it could be negligible. In the SEM image of Fig. 3(c) and Fig. 3(d), the formation of SiO_2 phase increased the average coating layer thickness of coated samples and several paths in coating layers were created along the length of the sample due to oxygen diffusion [11]. For sample D, after the thermal shock test, the coating layer was completely detached from the C/C substrate. An aperture was formed between the detached coating part and substrate, which accelerated the weight loss of carbon composites, and carbon sources were exhausted. However, for RD, the coating layer did not separate from the C/C substrate, and carbon sources of the composites did not disappear easily.

This phenomenon occurs due to the thermal stress (σ) of coated composites during the thermal shock test. There is a mismatch of thermal expansion between the C/C substrate and the coating layer, and it is calculated by Eq. (1) [12]:

$$\sigma = (\alpha_2 - \alpha_1) \Delta T \frac{E_2}{1-\mu_1} \frac{1}{1 + \frac{H_2}{H_1} \frac{E_2}{E_1} \frac{1-\mu_1}{1-\mu_2}} \qquad (1)$$

where, α is coefficient of thermal expansion, E is Young's modulus, μ is Poisson's ratio, H is the thickness of the material, and ΔT is the temperature difference. The subscripts 1 and 2 indicate the properties of carbon composites and SiC coating layer, respectively. Table 2 displays the values for μ, E, and α based on previous reports [13-17]. The calculated thermal stress of sample D and RD was 4254 and 4186 MPa, respectively. This thermal stress induces residual tensile stress during cooling because the thermal expansion coefficient of the SiC-coated layer is greater than that of the C/C substrate. The detachment of the SiO_2 coating layer in sample D can be attributed to the adhesive bond strength of CVD coating, which cannot endure residual tensile stress. Applying CVR coating before the CVD

TABLE 2

Parameter values for calculating thermal stress

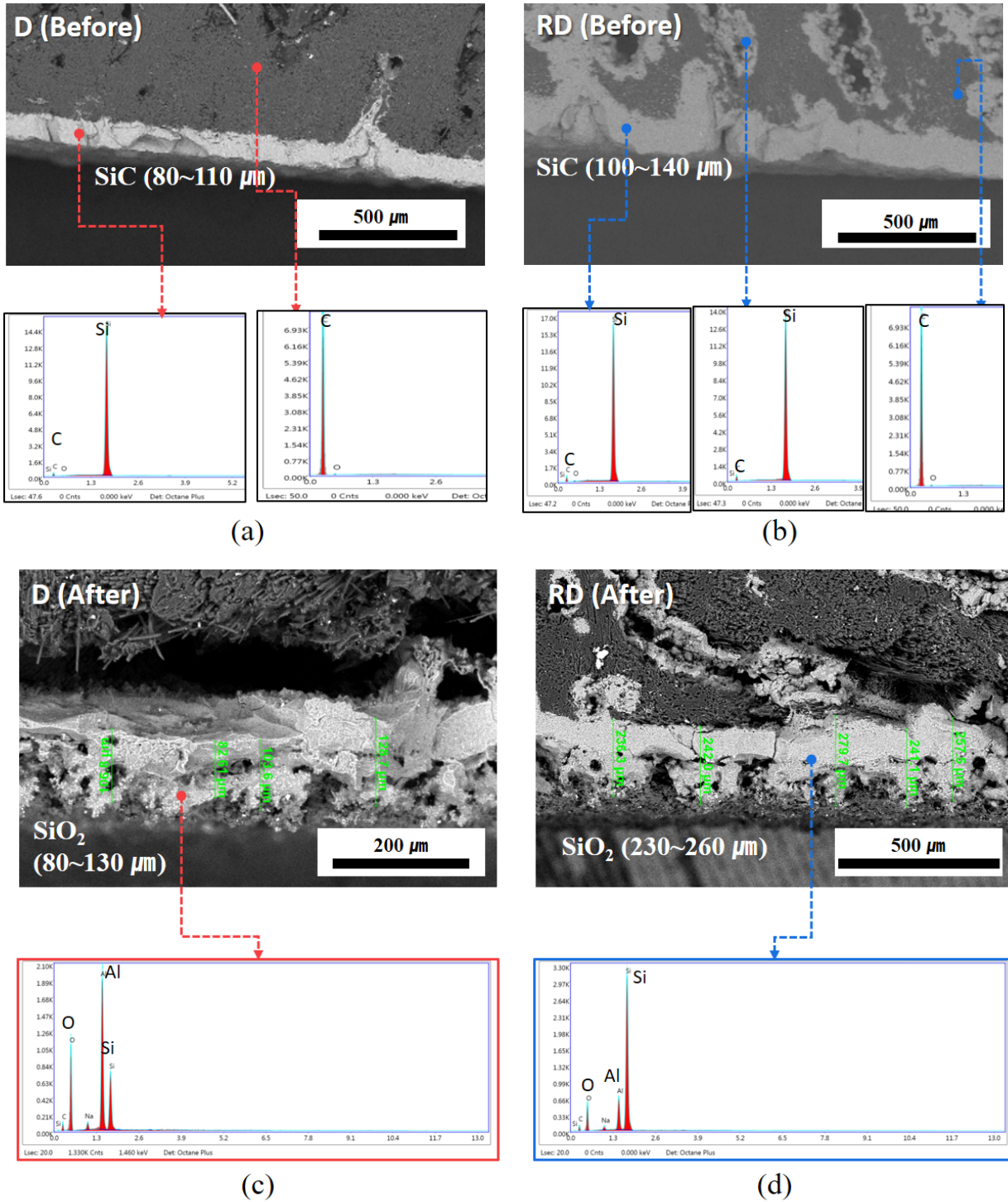| Parameter	Value
α_1	-0.74×10^{-6} /K
α_2	-0.74×10^{-6} /K
E_1	210×10^9 N/m^2
E_2	450×10^9 N/m^2
μ_1	0.307
μ_2	0.142
H_1	5×10^{-3} m
H_2	D: 0.105×10^{-3} m, RD: 0.120×10^{-3} m

Fig. 3. Cross-sectional SEM/EDS images of coated samples before/after the thermal shock test: (a) D and (b) RD before the test, (c) D and (d) RD after the test

coating improves the adhesive strength between the coating layer and the C/C substrate by endowing roughness to carbon composites [5]. The crack propagation visible in Fig. 2 can be induced from the residual tensile strength and detachment of the coating layer in sample D. Applying CVR coating before CVD coating effectively improves thermal durability and the service life of carbon composites.

Fig. 4 shows that the spherical indentation test was performed before and after the thermal shock to evaluate mechanical properties and wear resistance. The elastic modulus is calculated using Eq. (2) [18]:

$$E = \frac{1}{2} \frac{dP}{dh} \frac{1}{R^{\frac{1}{2}} h_e^{\frac{1}{2}}} \tag{2}$$

where E is elastic modulus, R is tip radius, and h_e is elastic depth. The difference of residual displacement (h_p) and maximum displacement (h_m) provides the value for elastic depth (h_e) (Fig. 4).

The hardness (H) is determined by dividing the load (P) by the surface area of indentation (A) as presented in Eq. (3), and this area is calculated using Eq. (4). [19]:

$$H = \frac{P}{A} \tag{3}$$

$$A = 24.5 h_p^2 \tag{4}$$

Fig. 5 shows the relative elastic modulus and hardness of D and RD. Before the thermal shock test, in sample RD, the relative elastic modulus and relative hardness were 29% and 37% higher, respectively, than that of sample D. After the thermal shock test, the elastic modulus and hardness of RD were 16% and 15%, respectively, higher than that of sample D. Performing the CVR process before the CVD process improves the elastic modulus and hardness of the sample. These effects remain after the conclusion of the thermal shock test.
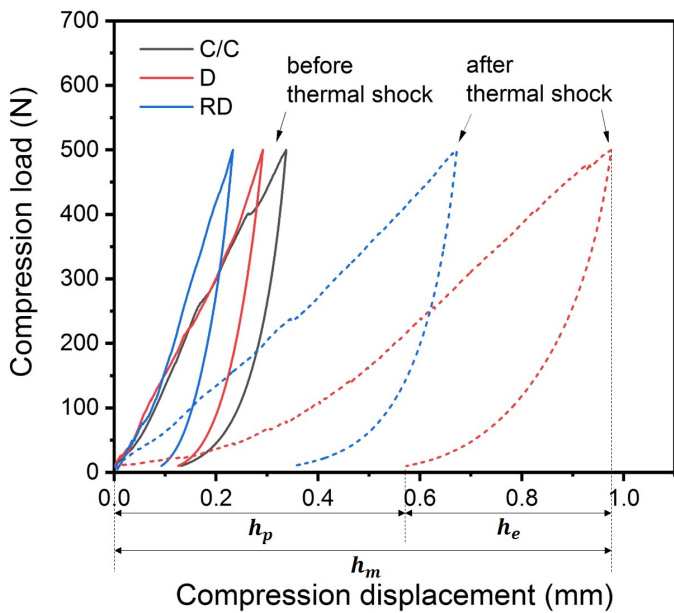

Fig. 4. Indentation load-displacement curves of uncoated and coated samples before/after the thermal shock test

4. Conclusions

The thermal durability and mechanical properties of the SiC-coated carbon composites were investigated in an oxidative environment. The CVD and the CVR process was used to deposit the coating on samples. After the thermal shock test, the weight remnant ratio of samples decreased with every cycle. After the test, the bare C/C samples nearly disappeared, and the remained weights of coated samples, D and RD, were 77.91% and 97.08%, respectively. The coating layer of RD was not detached after the thermal shock test because RD endured the thermal stress (4186 MPa). The relative elastic modulus and the relative hardness of the sample RD were higher than those of D, even after the thermal shock test. These results show that performing the CVR process before the CVD coating effectively improves the thermal durability and mechanical properties of carbon composites in oxidative surroundings.
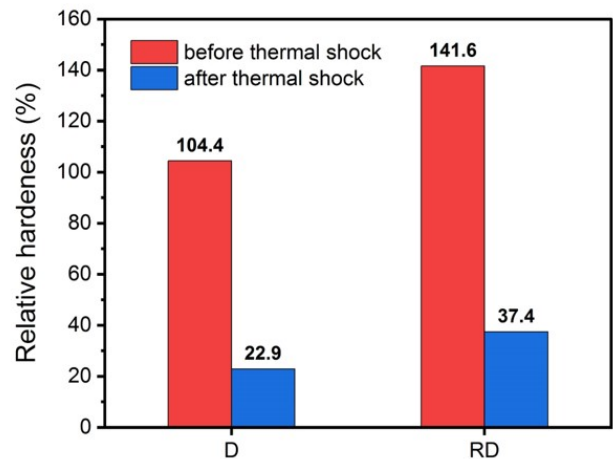
REFERENCES

[1] S.J. Park, M.K. Seo, Interface Science and Composites: Volume **18**, Academic Press; 1st Edition (2011).

[2] X. Zhu, Z. Yang, H. Li, M. Kang, Proceedings of ICCM-10, Whistler (1995).

[3] X. Qiang, H. Li, Y. Zhang, D. Yao, L. Guo, J. Wei, Corros. Sci. **59**, 343-347 (2012). DOI:10.1016/j.corsci.2012.01.035

[4] W. Shi, Y. Tan, J. Hao, J. Li, Ceram. Int. **42** (15), 17666-17672 (2016). DOI: 10.1016/j.ceramint.2016.08.083
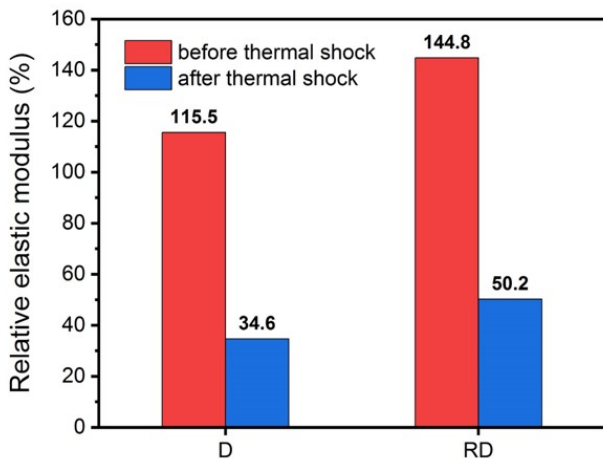
(a)

(b)

Fig. 5. (a) Relative elastic modulus and (b) relative hardness of coated samples before/after the thermal shock

[5] S.B. Bae, J.E. Lee, J.G. Paik, N.C. Cho, H.I. Lee, Arch. Metall. Mater. **65** (4), 1371-1375 (2020).

[6] S.D. Choi, H.I. Seo, B.J. Lim, I.C. Sihn, J.M. Lee, J.K. Park, K.S. Lee, Compos. Res. **31** (5), 260-266 (2018).

[7] K.S. Lee, Z. Meng, I.C. Sihn, K. Choi, J.E. Lee, S.B. Bae, H.I. Lee, Ceram. Int. **46** (13), 21233-21242 (2020). DOI:10.1016/j.ceramint.2020.05.211

[8] D.H. Lee, K.S. Lee, T.W. Kim, C. Kim, Ceram. Int. **45** (17), 21348-21358 (2019). DOI:10.1016/j.ceramint.2019.07.121

[9] Z. Li, X. Yin, T. Ma, W. Miao, Z. Zhang, Mater. Trans. **52** (12), 2165-2167 (2011). DOI:10.2320/matertrans.MAW201103

[10] P.J. Jorgensen, M.E. Wardsworths, I.B. Cuter, J. Am. Cer. Soc. **42** (12), 613-616 (1959). DOI:10.1111/j.1151-2916.1959.tb13582.x

[11] A. Abdollahi, N. Ehsani, Metall. Mater. Trans. A. **48**, 265-278 (2017). DOI:10.1007/s11661-016-3813-z

[12] K.S. Lee, D.K. Kim, S.K. Lee, B.R. Lawn, J. Korean Ceram. **4** (4), 356-362 (1998).

[13] http://www.tanxw.com/news/xgzx/1654.html, accessed: 26.08.2020.

[14] http://www.360doc.com/content/19/1014/10/9122134_866684074.shtml, accessed: 26.08.2020.

[15] http://cn.chinatungsten.com/Si/thgdxz.html, accessed: 26.08.2020.

[16] https://blog.csdn.net/dxuehui/article/details/52497907, accessed: 26.08.2020.

[17] http://cn.chinatungsten.com/Si/thgdxz.html, accessed: 26.08.2020.

[18] A. Tiwari, S. Natarajan, Applied Nanoindentation in Advanced Materials, John Wiley & Sons (2017). DOI:10.1002/9781119084501

[19] G.C. Shwartz, K.V. Srikrishnan, Handbook of Semiconductor Interconnection Technology, CRC Press (2006). DOI:10.1201/9781420017656